CLNS 95/1372
CLEO 95-20

Measurement of the Form Factors for $\bar{B}^0 \to D^{*+}\ell^-\bar{\nu}$

J.E. Duboscq,[1] R. Fulton,[1] D. Fujino,[1] K.K. Gan,[1] K. Honscheid,[1] H. Kagan,[1] R. Kass,[1] J. Lee,[1] M. Sung,[1] C. White,[1] R. Wanke,[1] A. Wolf,[1] M.M. Zoeller,[1] X. Fu,[2] B. Nemati,[2] S.J. Richichi,[2] W.R. Ross,[2] P. Skubic,[2] M. Wood,[2] M. Bishai,[3] J. Fast,[3] E. Gerndt,[3] J.W. Hinson,[3] T. Miao,[3] D.H. Miller,[3] M. Modesitt,[3] E.I. Shibata,[3] I.P.J. Shipsey,[3] P.N. Wang,[3] L. Gibbons,[4] S.D. Johnson,[4] Y. Kwon,[4] S. Roberts,[4] E.H. Thorndike,[4] C.P. Jessop,[5] K. Lingel,[5] H. Marsiske,[5] M.L. Perl,[5] S.F. Schaffner,[5] R. Wang,[5] T.E. Coan,[6] J. Dominick,[6] V. Fadeyev,[6] I. Korolkov,[6] M. Lambrecht,[6] S. Sanghera,[6] V. Shelkov,[6] R. Stroynowski,[6] I. Volobouev,[6] G. Wei,[6] M. Artuso,[7] A. Efimov,[7] M. Gao,[7] M. Goldberg,[7] D. He,[7] N. Horwitz,[7] S. Kopp,[7] G.C. Moneti,[7] R. Mountain,[7] Y. Mukhin,[7] S. Playfer,[7] T. Skwarnicki,[7] S. Stone,[7] X. Xing,[7] J. Bartelt,[8] S.E. Csorna,[8] V. Jain,[8] S. Marka,[8] D. Gibaut,[9] K. Kinoshita,[9] P. Pomianowski,[9] S. Schrenk,[9] B. Barish,[10] M. Chadha,[10] S. Chan,[10] G. Eigen,[10] J.S. Miller,[10] C. O'Grady,[10] M. Schmidtler,[10] J. Urheim,[10] A.J. Weinstein,[10] F. Würthwein,[10] D.M. Asner,[11] M. Athanas,[11] D.W. Bliss,[11] W.S. Brower,[11] G. Masek,[11] H.P. Paar,[11] J. Gronberg,[12] C.M. Korte,[12] R. Kutschke,[12] S. Menary,[12] R.J. Morrison,[12] S. Nakanishi,[12] H.N. Nelson,[12] T.K. Nelson,[12] C. Qiao,[12] J.D. Richman,[12] D. Roberts,[12] A. Ryd,[12] H. Tajima,[12] M.S. Witherell,[12] R. Balest,[13] K. Cho,[13] W.T. Ford,[13] M. Lohner,[13] H. Park,[13] P. Rankin,[13] J. Roy,[13] J.G. Smith,[13] J.P. Alexander,[14] C. Bebek,[14] B.E. Berger,[14] K. Berkelman,[14] K. Bloom,[14] D.G. Cassel,[14] H.A. Cho,[14] D.M. Coffman,[14] D.S. Crowcroft,[14] M. Dickson,[14] P.S. Drell,[14] D.J. Dumas,[14] R. Ehrlich,[14] R. Elia,[14] P. Gaidarev,[14] B. Gittelman,[14] S.W. Gray,[14] D.L. Hartill,[14] B.K. Heltsley,[14] C.D. Jones,[14] S.L. Jones,[14] J. Kandaswamy,[14] N. Katayama,[14] P.C. Kim,[14] D.L. Kreinick,[14] T. Lee,[14] Y. Liu,[14] G.S. Ludwig,[14] J. Masui,[14] J. Mevissen,[14] N.B. Mistry,[14] C.R. Ng,[14] E. Nordberg,[14] J.R. Patterson,[14] D. Peterson,[14] D. Riley,[14] A. Soffer,[14] C. Ward,[14] P. Avery,[15] A. Freyberger,[15] C. Prescott,[15] S. Yang,[15] J. Yelton,[15] G. Brandenburg,[16] R.A. Briere,[16] D. Cinabro,[16] T. Liu,[16] M. Saulnier,[16] R. Wilson,[16] H. Yamamoto,[16] T. E. Browder,[17] F. Li,[17] J. L. Rodriguez,[17] T. Bergfeld,[18] B.I. Eisenstein,[18] J. Ernst,[18] G.E. Gladding,[18] G.D. Gollin,[18] M. Palmer,[18] M. Selen,[18] J.J. Thaler,[18] K.W. Edwards,[19] K.W. McLean,[19] M. Ogg,[19] A. Bellerive,[20] D.I. Britton,[20] R. Janicek,[20] D.B. MacFarlane,[20] P.M. Patel,[20] B. Spaan,[20] A.J. Sadoff,[21] R. Ammar,[22] P. Baringer,[22] A. Bean,[22] D. Besson,[22] D. Coppage,[22] N. Copty,[22] R. Davis,[22] N. Hancock,[22] S. Kotov,[22] I. Kravchenko,[22] N. Kwak,[22] Y. Kubota,[23] M. Lattery,[23] J.K. Nelson,[23] S. Patton,[23] R. Poling,[23] T. Riehle,[23] V. Savinov,[23] M.S. Alam,[24] I.J. Kim,[24] Z. Ling,[24] A.H. Mahmood,[24] J.J. O'Neill,[24] H. Severini,[24] C.R. Sun,[24] S. Timm,[24] and F. Wappler[24]

(CLEO Collaboration)

[1]*Ohio State University, Columbus, Ohio, 43210*
[2]*University of Oklahoma, Norman, Oklahoma 73019*
[3]*Purdue University, West Lafayette, Indiana 47907*
[4]*University of Rochester, Rochester, New York 14627*
[5]*Stanford Linear Accelerator Center, Stanford University, Stanford, California, 94309*
[6]*Southern Methodist University, Dallas, Texas 75275*
[7]*Syracuse University, Syracuse, New York 13244*
[8]*Vanderbilt University, Nashville, Tennessee 37235*
[9]*Virginia Polytechnic Institute and State University, Blacksburg, Virginia, 24061*
[10]*California Institute of Technology, Pasadena, California 91125*
[11]*University of California, San Diego, La Jolla, California 92093*
[12]*University of California, Santa Barbara, California 93106*
[13]*University of Colorado, Boulder, Colorado 80309-0390*
[14]*Cornell University, Ithaca, New York 14853*
[15]*University of Florida, Gainesville, Florida 32611*
[16]*Harvard University, Cambridge, Massachusetts 02138*
[17]*University of Hawaii at Manoa, Honolulu, HI 96822*
[18]*University of Illinois, Champaign-Urbana, Illinois, 61801*
[19]*Carleton University, Ottawa, Ontario K1S 5B6 and the Institute of Particle Physics, Canada*
[20]*McGill University, Montréal, Québec H3A 2T8 and the Institute of Particle Physics, Canada*
[21]*Ithaca College, Ithaca, New York 14850*
[22]*University of Kansas, Lawrence, Kansas 66045*
[23]*University of Minnesota, Minneapolis, Minnesota 55455*
[24]*State University of New York at Albany, Albany, New York 12222*

Abstract

Using a sample of 2.6×10^6 $\Upsilon(4S) \to B\bar{B}$ events collected with the CLEO II detector at the Cornell Electron Storage Ring, we have measured the form factors for $\bar{B}^0 \to D^{*+}\ell^-\overline{\nu}$. We perform a three-parameter fit to the joint distribution of four kinematic variables to obtain the form factor ratios $R_1 = 1.18 \pm 0.30 \pm 0.12$ and $R_2 = 0.71 \pm 0.22 \pm 0.07$, and the form-factor slope $\rho^2_{A_1} = 0.91 \pm 0.15 \pm 0.06$, which is closely related to the slope of the Isgur-Wise function. The form factor ratios are consistent with predicted corrections to the heavy-quark symmetry limit of $R_1 = R_2 = 1$.

PACS numbers: 13.20.He, 12.39.Hg, 12.38.Qk

Semileptonic decays of hadrons containing a bottom quark provide a means both to measure fundamental parameters of the standard model—the magnitudes of the Cabibbo-Kobayashi-Maskawa mixing angles V_{cb} and V_{ub}—and to understand the effects of strong interactions on the underlying weak decays. These two problems are related, because accurate determination of CKM elements requires a good understanding of the decay dynamics [1]. The decay $B \to D^* \ell \nu$ is a key process for these studies. It has been analyzed in detail [2–9] in the framework of heavy quark effective theory (HQET), in which the decay amplitude is expanded in powers of $1/m_b$ and $1/m_c$. Because the charm and bottom quark masses are reasonably large compared with the energies associated with strong interactions in the decay, both the masses and the spins of the heavy quarks are expected to play little role in the dynamics. These considerations lead to symmetry relations that significantly simplify the description of the process. For $B \to D^* \ell \nu$, HQET yields numerous predictions, some of which we are able to test using the detailed studies of decay distributions presented in this paper.

In calculations of exclusive semileptonic decays, the amplitude is expressed in terms of the available four vectors and one or more form factors, which are Lorentz-invariant functions that depend only on q^2, the square of the mass of the virtual W. The form factors parametrize the effect of strong interactions on the decay. The decay $B \to D^* \ell \nu$ ($\ell = e,\ \mu$) depends on three form factors. Although HQET does not predict their q^2 dependence, it does relate these form factors, up to relatively small corrections, to a single, universal form factor, called the Isgur-Wise function, which is predicted by nonperturbative methods such as lattice QCD and QCD sum rules [10]. The goal of this analysis is to test the predictions of both HQET and these nonperturbative methods.

We study the form factors for $\bar{B}^0 \to D^{*+} \ell^- \overline{\nu}$ (charge-conjugate modes are implied throughout this paper) using the channel $D^{*+} \to D^0 \pi^+$ with $D^0 \to K^- \pi^+$ or $D^0 \to K^- \pi^+ \pi^0$. The integrated luminosity of the data sample is 2.404 fb^{-1} on the $\Upsilon(4S)$, which corresponds to $(2.579 \pm 0.018) \times 10^6$ $B\bar{B}$ pairs. The data were collected using the CLEO II detector, which is described elsewhere [11].

The differential decay rate for $\bar{B}^0 \to D^{*+} \ell^- \overline{\nu}$, $D^{*+} \to D^0 \pi^+$ can be expressed in terms of three q^2-dependent helicity amplitudes $H_\pm(q^2)$ and $H_0(q^2)$, where the subscripts refer to the helicity of either the virtual W or the D^{*+}. The rate is given by

$$
\begin{aligned}
\frac{d\Gamma(\bar{B}^0 \to D^{*+} \ell^- \overline{\nu},\ D^{*+} \to D^0 \pi^+)}{dq^2\, d\cos\theta_\ell\, d\cos\theta_V\, d\chi} &= \frac{3 G_F^2 |V_{cb}|^2\, P_{D^*}\, q^2}{8(4\pi)^4 M^2} \mathcal{B}(D^{*+} \to D^0 \pi^+) \times \\
&\{[(1-\cos\theta_\ell)^2 |H_+(q^2)|^2 + (1+\cos\theta_\ell)^2 |H_-(q^2)|^2] \sin^2\theta_V \\
&+ 4\sin^2\theta_\ell \cos^2\theta_V |H_0(q^2)|^2 - 2\sin^2\theta_\ell \sin^2\theta_V \cos(2\chi) H_+(q^2) H_-(q^2) \\
&+ 4\sin\theta_\ell \sin\theta_V \cos\theta_V \cos\chi\, H_0(q^2)[\cos\theta_\ell (H_-(q^2) + H_+(q^2)) + (H_-(q^2) - H_+(q^2))]\},
\end{aligned}
\tag{1}
$$

where M is the mass of the B meson; P_{D^*} is the momentum of the D^* in the B rest frame and is a function of q^2; $\mathcal{B}(D^{*+} \to D^0 \pi^+)$ is the branching fraction for $D^{*+} \to D^0 \pi^+$; θ_ℓ is the decay angle of the lepton in the virtual W rest frame; θ_V is the decay angle of the D^0 in the D^* rest frame; and χ is the angle between the decay planes of the W and the D^* in the B rest frame [1]. Although the distributions of some of these variables have been studied previously [12–15], our analysis is the first to use all four variables (q^2, $\cos\theta_\ell$, $\cos\theta_V$, and χ), and it is the first to use their correlations, which are quite powerful.

The helicity amplitudes $H_\pm$ and H_0 can be expressed in terms of two axial-vector form factors, $A_1(q^2)$ and $A_2(q^2)$, and a vector form factor $V(q^2)$:

$$\begin{aligned} H_\pm(q^2) &= (M+m)A_1(q^2) \mp \frac{2M\,P_{D^*}}{(M+m)}V(q^2), \\ H_0(q^2) &= \frac{1}{2m\sqrt{q^2}}\Big[(M^2-m^2-q^2)(M+m)A_1(q^2) - \frac{4M^2\,P_{D^*}^2}{(M+m)}A_2(q^2)\Big], \end{aligned} \tag{2}$$

where m is the mass of the D^* meson.

In the heavy-quark symmetry limit ($m_c,\ m_b \to \infty$), the form factors are related to the Isgur-Wise function ξ:

$$V(q^2) = A_2(q^2) = \frac{A_1(q^2)}{\left[1 - \dfrac{q^2}{(M+m)^2}\right]} = \frac{(M+m)}{2\sqrt{Mm}}\xi(w), \tag{3}$$

where $w = (M^2+m^2-q^2)/(2Mm)$. The variable w is simply the relativistic factor γ of the D^* in the B-meson rest frame and is sometimes called y. Following Neubert [6], we define the form factor ratios

$$\begin{aligned} R_1(w) &\equiv \left[1 - \frac{q^2}{(M+m)^2}\right]\frac{V(q^2)}{A_1(q^2)}, \\ R_2(w) &\equiv \left[1 - \frac{q^2}{(M+m)^2}\right]\frac{A_2(q^2)}{A_1(q^2)}. \end{aligned} \tag{4}$$

These ratios are predicted to be unity, independent of w, in the heavy-quark symmetry limit.

To allow departures from the heavy-quark symmetry limit but still express the form factors in a manner that makes this limit transparent, one can use

$$\begin{aligned} A_1(q^2) &= \frac{M+m}{2\sqrt{Mm}}\left[1 - \frac{q^2}{(M+m)^2}\right]h_{A_1}(w), \\ A_2(q^2) &= \frac{M+m}{2\sqrt{Mm}}R_2(w)h_{A_1}(w), \\ V(q^2) &= \frac{M+m}{2\sqrt{Mm}}R_1(w)h_{A_1}(w), \end{aligned} \tag{5}$$

where $h_{A_1}(w) \to \xi(w)$, $R_1(w) \to 1$, and $R_2(w) \to 1$ in the heavy-quark symmetry limit, recovering Eq. (3). Departures from this limit produce two effects: deviations of $R_1(1)$ and $R_2(1)$ from unity and a slight variation of R_1 and R_2 with w.

Since the range of D^* recoil velocities is small ($w-1 \leq 0.5$), the form factors are expected to have approximately linear behavior. We fit for the slope of $h_{A_1}(w)$, assuming the linear form

$$h_{A_1}(w) = h_{A_1}(1)[1 - \rho^2_{A_1}(w-1)]. \tag{6}$$

We assume that R_1 and R_2 are constant, so that the free parameters in the fit are R_1, R_2, and $\rho^2_{A_1}$. In reality, R_1 and R_2 are expected to have a mild dependence on w [6,9]. We will test the sensitivity of our results to these assumptions by performing alternative fits using different forms for $R_1(w)$, $R_2(w)$, and $h_{A_1}(w)$.

We select events with at least one electron candidate with momentum in the range 1.0 GeV/c to 2.45 GeV/c, or at least one muon candidate with momentum in the range 1.4 GeV/c to 2.45 GeV/c. We reconstruct D^{*+}'s in the mode $D^{*+} \to D^0\pi^+$ with $D^0 \to K^-\pi^+$ or $D^0 \to K^-\pi^+\pi^0$; the reconstructed D^{*+}–D^0 mass difference, δm, is required to be within 2 MeV/c^2 of the nominal value. Complete details of the event selection will be given elsewhere [16].

Table I lists the estimated number of events from each background and the signal. The largest background, fake D^*'s (combinatorial background under the D^* peak), is only 10% of the signal. The background from $B \to D^{**}\ell\nu$, $D^{**} \to D^{*+}\pi$, though even smaller, has a larger uncertainty, since there are several D^{**} states, and their contributions have not been well measured. Our model for this background source is based on a combination of measurements from ALEPH [17] and predictions from the ISGW2 model [18]. The background from events in which the lepton and the D^{*+} are produced in the decay chains of different B's (uncorrelated background) was determined directly from the data and is small. Fake lepton backgrounds are determined from measured probabilities for hadrons to fake lepton signatures, and the continuum background is determined using off-resonance data.

The joint distribution in q^2, $\cos\theta_\ell$, $\cos\theta_V$, and χ is fit using the unbinned maximum likelihood method. To incorporate detector smearing and acceptance effects, we use a Monte Carlo technique [19] to evaluate the likelihood function.

Since fake D^*'s are the largest background they are explicitly included in the fit, as is the background from the uncorrelated D^*–lepton events. The $B \to D^{**}\ell\nu$ background is treated differently: a term is not included directly in the fitting function, but we use Monte Carlo events to evaluate a small systematic shift that is caused by omitting this background in the fit.

Figures 1(a) and 1(b) show the data and fit distributions for q^2 and $\cos\theta_\ell$. Figures 1(c) and 1(d) show the distributions that would be observed by a perfect detector, assuming the values of the parameters obtained from the fit.

Figures 2(a) and 2(b) show the observed distributions for $\cos\theta_V$ in two q^2 bins. At low q^2, the lepton and neutrino are nearly parallel, forcing the D^* to have helicity zero; this in turn introduces a strong $\cos^2\theta_V$ component in this region of phase space. As q^2 increases, the other helicity components contribute as well, and at $q^2_{\rm max}$ the D^* must be unpolarized.

Figures 2(c) and 2(d) show an interesting correlation between $\cos\theta_V$ and χ, produced by the interference term proportional to $(H_+(q^2) - H_-(q^2))H_0(q^2)$. The difference between H_+ and H_- results from the higher probability for the daughter c-quark to have helicity $-1/2$ than helicity $+1/2$. If the coupling at the W vertices were $(V \mp A) \times (V \pm A)$ the slopes in Figures 2(c) and 2(d) would be reversed; for $(V \pm A) \times (V \pm A)$ the slopes would be as we observe.

All observed distributions are described well by the fit. The values of R_1, R_2, and $\rho^2_{A_1}$ that we obtain are given in the first entry in Table II. The other entries in Table II summarize the results of the alternative fits. Alternative forms of $h_{A_1}(w)$ yield higher values of $\rho^2_{A_1}$ (which specifies the slope at $w = 1$ in all cases), while the extracted values of R_1 and R_2 are only mildly changed for the fits with alternative forms of $h_{A_1}(w)$.

The systematic errors on the fit results are given in Table III. The uncertainty on the slow-pion efficiency primarily affects the q^2 distribution, which in turn affects $\rho^2_{A_1}$. To evaluate the likelihood function, we count weighted Monte Carlo events in a four-dimensional volume constructed around each data point. This method results in a small bias due to the nonzero volume size. We correct for this bias and include an uncertainty in the correction. We also include an uncertainty due to the finite size of the Monte Carlo sample. The uncertainty in modeling $B \to D^{**}\ell\nu$ affects R_1, since the soft lepton spectrum of these events modifies the $\cos\theta_\ell$ distribution. The uncertainty on the lepton-identification efficiency as a function of momentum is quite small, as is the uncertainty associated with the uncorrelated background. Finally, there is an uncertainty in using the δm sideband to model the combinatorial background under the D^* peak.

From these results, we can derive $\bar{A}_{\rm FB}$, the lepton forward-backward asymmetry, and $\bar{A}_{\rm pol}$, the D^* polarization, which are both defined in Ref. [6]. Using the values from the linear fit, we obtain $\bar{A}_{\rm FB} = 0.197 \pm 0.033 \pm 0.016$ and $\bar{A}_{\rm pol} = 1.55 \pm 0.26 \pm 0.13$, consistent with, but more precise than previous results [12,14]. For the value $\rho^2_{A_1} = 0.9$, Neubert calculates [6] $\bar{A}_{\rm FB} = 0.22$ and $\bar{A}_{\rm pol} = 1.40$.

In conclusion, we have measured the form factors for the process $\bar{B}^0 \to D^{*+}\ell^-\overline{\nu}$ using an unbinned maximum likelihood fit. We obtain the form factor ratios $R_1 = 1.18 \pm 0.30 \pm 0.12$ and $R_2 = 0.71 \pm 0.22 \pm 0.07$, which can be compared with the heavy-quark symmetry limit of $R_1 = R_2 = 1$. Our values agree with the predictions of Neubert [6], $R_1(1) = 1.35$ and $R_2(1) = 0.79$, Close and Wambach [9], $R_1(1) = 1.15$ and $R_2(1) = 0.91$, and the ISGW2 model [18], $R_1(1) = 1.27$ and $R_2(1) = 1.01$. In the same fit, we determine the slope of $h_{A_1}(w)$ to be $\rho^2_{A_1} = 0.91 \pm 0.15 \pm 0.06$. Since we assume a linear form, this parameter measures the average slope over the w range. This value is in the range expected from lattice QCD and QCD sum rules [10]. We also find that R_1 and R_2 are not sensitive either to the form of $h_{A_1}(w)$ or the w dependence, as indicated by theory, of the form factor ratios. However, $\rho^2_{A_1}$ is found to be sensitive to the form of $h_{A_1}(w)$ used. Alternative forms, with positive curvature, give higher values of $\rho^2_{A_1}$, the slope at $w = 1$.

The comparison of this measurement of $\rho^2_{A_1}$ with that from the CLEO II $|V_{cb}|$ measurement [15] using $B \to D^*\ell\nu$ requires some care. That measurement uses a procedure in which the $d\Gamma/dq^2$ distribution is fit to a function that assumes $R_1 = R_2 = 1$. For this reason, it is common to refer to the slope parameter obtained from this procedure as $\hat{\rho}^2$. Neubert provides a relation [7] between $\hat{\rho}^2$ and $\rho^2_{A_1}$ as a function of R_1 and R_2, from which we obtain $\rho^2_{A_1} \approx \hat{\rho}^2 + 0.22$. The CLEO II value of $\hat{\rho}^2$ is $0.84 \pm 0.13 \pm 0.08$, which would correspond to a value of $\rho^2_{A_1}$ around 1.06. Thus, the CLEO II $\rho^2_{A_1}$ and $\hat{\rho}^2$ measurements, which are essentially statistically independent, are consistent.

One of the results of our fit is that the corrections to the heavy-quark symmetry limit do indeed appear to be fairly small. This result provides some confidence in the use of heavy-quark symmetry as a starting point for the extraction of $|V_{cb}|$ from $B \to D^*\ell\nu$.

We gratefully acknowledge the effort of the CESR staff in providing us with excellent luminosity and running conditions. This work was supported by the National Science Foundation, the U.S. Department of Energy, the Heisenberg Foundation, the Alexander von Humboldt Stiftung, the Natural Sciences and Engineering Research Council of Canada, and the A.P. Sloan Foundation.

REFERENCES

[1] J. Richman and P. Burchat, to be published in Rev. Mod. Phys. (1995), UCSB preprint UCSB-HEP-95-08.

[2] N. Isgur and M.B. Wise, Phys. Lett. B **232**, 113 (1989).

[3] N. Isgur and M.B. Wise, Phys. Lett. B **237**, 527 (1990).

[4] M. Neubert, Phys. Lett. B **264**, 455 (1991).

[5] M. Neubert and V. Rieckert, Nucl. Phys. B **382**, 97 (1992).

[6] M. Neubert, Phys. Reports **245**, 259 (1994).

[7] M. Neubert, Phys. Lett. B **338**, 84 (1994).

[8] M. Shifman, N.G. Uraltsev, and A. Vainshtein, Phys. Rev. D **51**, 2217 (1995).

[9] F.E. Close and A. Wambach, Phys. Lett. B **348**, 207 (1995).

[10] S.P. Booth, *et al.* (UKQCD), Phys. Rev. Lett. **72**, 462 (1994); C. Bernard, Y. Shen, and A. Soni, Phys. Lett. B **317**, 164 (1993); B. Blok and M. Shifman, Phys. Rev. D **47**, 2949 (1993); other predictions are summarized in Ref. [1].

[11] Y. Kubota *et al.* (CLEO), Nucl. Instrum. Methods Phys. Res., Sect. A **320**, 66 (1992).

[12] H. Albrecht *et al.* (ARGUS), Z. Phys. C **57**, 533 (1993).

[13] D. Bortoletto, *et al.* (CLEO), Phys. Rev. Lett. **63**, 1667 (1989).

[14] S. Sanghera *et al.* (CLEO), Phys. Rev. D **47**, 791 (1993).

[15] B. Barish *et al.* (CLEO), Phys. Rev. D **51**, 1014 (1995).

[16] CLEO Collab., to be submitted to Phys. Rev. D, see also CLEO-CONF 95-27 submitted to the International Europhysics Conference on High Energy Physics, Brussels, Belgium, July 27 - August 2, 1995.

[17] D. Buskulic *et al.* (ALEPH), Phys. Lett. B **345**, 103 (1995).

[18] D. Scora and N. Isgur, Phys. Rev. D **52**, 2783 (1995).

[19] D.M. Schmidt, R.M. Morrison, and M. Witherell, Nucl. Instrum. Methods Phys. Res., Sect. A **328**, 547 (1993).

TABLES

	$K\pi\ e$	$K\pi\ \mu$	$K\pi\pi^0\ e$	$K\pi\pi^0\ \mu$	Total
Raw yield	267±16	292±17	192±14	189±14	940±31
Fake D^*	17± 3	21± 4	20± 4	21± 4	79± 8
$B \to D^{**}\ell\nu$	12± 7	17± 8	8± 5	11± 5	48±25
Uncorrelated	7± 4	3± 3	6± 3	0± 2	16± 6
Fake leptons	1± 1	6± 3	1± 1	5± 3	13± 6
Continuum	2± 2	3± 3	0± 2	0± 2	5± 5
Signal	228±18	242±20	157±16	152±16	779±42

TABLE I. The yields in the $K\pi$ and $K\pi\pi^0$ channels and the estimated background contributions. The different sources of background are explained in the text.

$h_{A_1}(w)/h_{A_1}(1)$	$R_1(w)$	$R_2(w)$	R_1	R_2	$\rho^2_{A_1}$
$1-\rho^2_{A_1}(w-1)$	R_1	R_2	$1.18 \pm 0.30 \pm 0.12$	$0.71 \pm 0.22 \pm 0.07$	$0.91 \pm 0.15 \pm 0.06$
$1-\rho^2_{A_1}(w-1)$	$R_1^{\rm Neub}(w)$	$R_2^{\rm Neub}(w)$	$1.24 \pm 0.30 \pm 0.12$	$0.65 \pm 0.22 \pm 0.07$	$0.91 \pm 0.15 \pm 0.06$
$1-\rho^2_{A_1}(w-1)$	$R_1^{\rm CW}(w)$	$R_2^{\rm CW}(w)$	$1.20 \pm 0.30 \pm 0.12$	$0.70 \pm 0.22 \pm 0.07$	$0.91 \pm 0.15 \pm 0.06$
$\exp[-\rho^2_{A_1}(w-1)]$	R_1	R_2	$1.21 \pm 0.32 \pm 0.12$	$0.72 \pm 0.22 \pm 0.07$	$1.27 \pm 0.29 \pm 0.12$
$\frac{2}{w+1}\exp[(1-2\rho^2_{A_1})\frac{w-1}{w+1}]$	R_1	R_2	$1.21 \pm 0.32 \pm 0.12$	$0.71 \pm 0.22 \pm 0.07$	$1.53 \pm 0.36 \pm 0.14$
$(\frac{2}{w+1})^{2\rho^2_{A_1}}$	R_1	R_2	$1.21 \pm 0.32 \pm 0.12$	$0.70 \pm 0.22 \pm 0.07$	$1.42 \pm 0.32 \pm 0.13$
$R_1^{\rm Neub}(w) = R_1[1-0.16(w-1)+0.07(w-1)^2]$			$R_2^{\rm Neub}(w) = R_2[1+0.19(w-1)+0.05(w-1)^2]$		
$R_1^{\rm CW}(w) = R_1[1-0.06(w-1)]$			$R_2^{\rm CW}(w) = R_2[1+0.04(w-1)]$		

TABLE II. Fits for the form factors with alternative forms of $h_{A_1}(w)$. The first entry in the table is the standard fit with a linear form of $h_{A_1}(w)$ and constant form factor ratios. The errors on the extracted parameters are correlated, the estimated correlations are $\rho_{R_1R_2} = -0.82$, $\rho_{R_1\rho^2} = 0.60$, and $\rho_{R_2\rho^2} = -0.80$. The next two entries have w dependent form factor ratios according to theoretical predictions. The last three entries use alternative forms of $h_{A_1}(w)$; the extracted values of $\rho^2_{A_1}$ are sensitive to these forms. The form factor ratios are not very sensitive to the form of $h_{A_1}(w)$.

	R_1	R_2	$\rho^2_{A_1}$
Slow-pion efficiency	0.01	0.01	0.04
Finite volumes	0.05	0.04	0.03
Finite MC statistics	0.03	0.01	0.01
$B \to D^{**}\ell\nu$	0.08	0.04	0.02
Lepton efficiency	0.02	0.02	0.01
Uncorr. Background	0.03	0.01	0.01
δm-sideband	0.05	0.03	0.03
Total	0.12	0.07	0.06

TABLE III. Systematic errors on R_1, R_2, and $\rho^2_{A_1}$ for the linear form of $h_{A_1}(w)$.

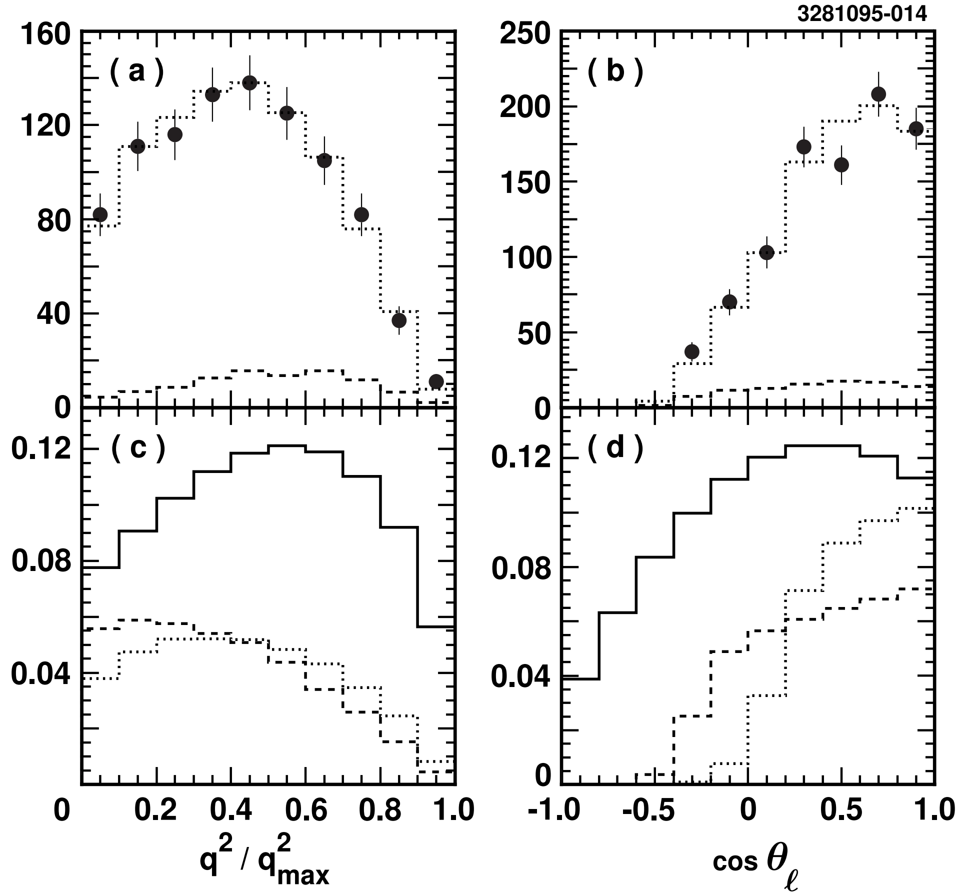

FIG. 1. The distributions of (a) q^2 and (b) $\cos\theta_\ell$ for data (points with error bars) and the fit (dotted histogram). The dashed line shows the contribution of the two backgrounds included in the fit. These histograms include both $D^0 \to K^-\pi^+$ and $D^0 \to K^-\pi^+\pi^0$ channels, electrons and muons. In (c) and (d), we show the distributions that would be observed by a perfect detector (solid) and the shapes of the acceptance for electrons (dashed curves) and muons (dotted curves). In (c) and (d) the vertical scale is arbitrary.

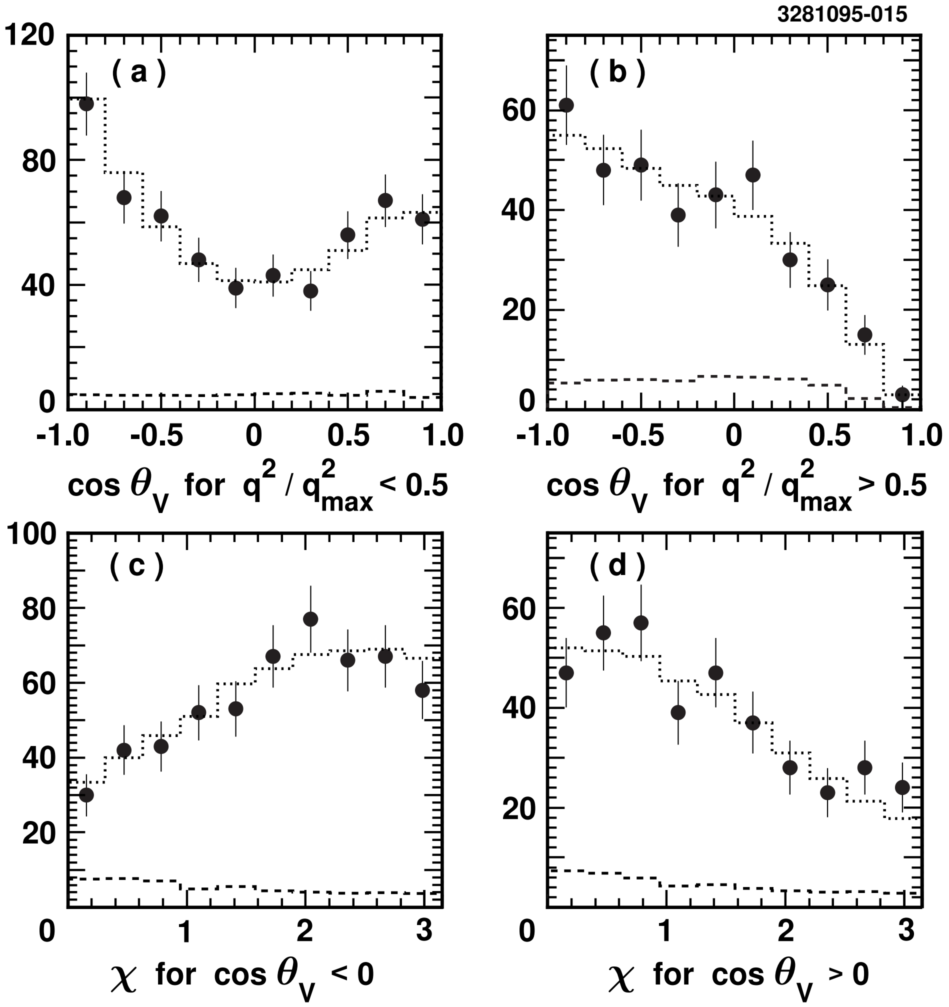

FIG. 2. Distributions of $\cos\theta_V$ for the (a) lower half and (b) upper half of the q^2 range. The dotted lines in the histograms show the result of the fit, and the dashed lines show the background. The lack of symmetry in $\cos\theta_V$ is due to poor acceptance for very slow pions. Figures (c) and (d) show the χ distributions for $\cos\theta_V < 0$ and $\cos\theta_V > 0$, respectively.